

Feasibility of Collagen Peptide-Based Wound Healing Applications – Final Report

Project code
2025-1101

Prepared by
Santanu Deb-Choudhury, Paul Middlewood, Stephen Haines, Mark Agasid, Sarah Fitzpatrick, Peter Smith, Marina Richena, Jeff Plowman, Robert Fletcher & Duane Harland

Date submitted
21/11/2025

Published by
XXXXXXX

Date published
XX/XX/XX

Contents

Contents	2
1.0 Abstract	3
2.0 Executive summary	4
3.0 Introduction	5
4.0 Project objectives	5
5.0 Methodology	6
6.0 Results	9
7.0 Discussion	17
8.0 Conclusions	20
9.0 Project outputs	21
10.0 Bibliography	21

Disclaimer The information contained within this publication has been prepared by a third party commissioned by Australian Meat Processor Corporation Ltd (AMPC). It does not necessarily reflect the opinion or position of AMPC. Care is taken to ensure the accuracy of the information contained in this publication. However, AMPC cannot accept responsibility for the accuracy or completeness of the information or opinions contained in this publication, nor does it endorse or adopt the information contained in this report.

No part of this work may be reproduced, copied, published, communicated or adapted in any form or by any means (electronic or otherwise) without the express written permission of Australian Meat Processor Corporation Ltd. All rights are expressly reserved. Requests for further authorisation should be directed to the Executive Chairman, AMPC, Suite 2, Level 6, 99 Walker Street North Sydney NSW.

1.0 Abstract

This project was undertaken to improve collagen-based wound dressings, which play an important role in wound care but currently face limitations in healing speed and sustainability. The aim was to develop improved bio-based materials by incorporating collagen peptides sourced from underutilised animal by-products, with a focus on Type III collagen, which is important for early-stage wound healing.

Collagen was extracted from sheep skin and lung tissue. Lung tissue provided a higher proportion of Type III collagen than skin. Enzymatic hydrolysis of lung collagen generated bioactive peptides, which were combined with skin-derived collagen, mainly Type I, to produce fibrous mats. These mats were tested with and without genipin crosslinking, showing open porous structures, good stability in simulated wound fluid, and no clear benefit of chemical crosslinking. Based on these results, non-crosslinked mats were selected for further testing. In a human 3D skin model, the collagen peptide-enriched dressings supported wound closure and tissue regeneration, confirming their potential as effective bioactive dressings.

An economic feasibility study showed that routine clinical dressings represent the most achievable initial market entry, offering favourable return on investment and moderate regulatory requirements. Trauma care and consumer plasters present longer-term opportunities as production scales and technology matures. High-cost biologics used in chronic wounds represent a niche but potentially high-value market, where differentiated collagen-based products could provide clinical and economic advantages. Freeze-drying was identified as the main cost driver, with potential savings achievable through optimisation.

This project demonstrates that animal by-products can be transformed into high-value wound care products, offering benefits for patient outcomes, industry profitability, and environmental sustainability.

2.0 Executive summary

Wound healing is a complex process requiring the coordinated interaction of cells, growth factors, and extracellular matrix (ECM) components. In cases of chronic or severe wounds, natural healing is impaired, driving the need for advanced wound care materials. Collagen-based dressings are widely used to promote healing; however, current products primarily rely on Type I collagen, which provides structural support but lacks the regenerative functions of Type III collagen that are critical during early healing. This project addressed the question: Can wound healing outcomes be enhanced by incorporating enzymatically derived Type III collagen peptides into collagen-based dressings, thereby improving tissue regeneration and cost-effectiveness?

The target audience includes the medical wound care sector (clinicians treating chronic and trauma wounds) and the biotechnology and red meat industries seeking sustainable, high-value uses for animal by-products. The findings will benefit industry stakeholders by demonstrating a value-add pathway to convert low-value meat co-products into advanced biomedical materials aligned with waste minimisation and sustainability goals, while also offering endogenous bioactives that are often absent from GMO-derived collagens.

Objectives

The project aimed to:

- Extract and characterise functional collagens from sheep by-products.
- Generate Type III collagen-enriched peptides and develop enhanced collagen wound dressings.
- Evaluate their biological performance and safety using 3D skin models.
- Conduct a preliminary financial feasibility and scalability assessment.

All objectives were achieved, confirming both technical feasibility and commercial potential.

Methodology

- Collagen was extracted from sheep skin and lung using a modified alkali process, followed by biochemical and structural characterisation.
- Peptides were produced enzymatically and identified by mass spectrometry.
- Collagen mats were fabricated, crosslinked with a natural crosslinker, genipin. Uncrosslinked and crosslinked samples were tested for mechanical stability and biodegradability in simulated wound fluid.
- Biological evaluation was carried out using a 3D full-thickness human skin burn model to assess healing, cytokine responses, and biocompatibility.
- A screening-level economic analysis assessed production costs, scalability, and market potential.

Key Findings

Collagen was successfully extracted from both skin and lung tissues, with the latter predominantly containing both Type I and III collagens. The enzymatically derived peptides were dominated by medium-to-high molecular weight fractions (1–10 kDa) and contained abundant Type III sequences relevant to early tissue repair. In 3D skin models, peptide-enriched collagen mats accelerated re-epithelialisation and balanced inflammatory responses compared to commercial collagen dressings. Economic analysis showed that pilot-scale production is feasible, with strong return on investment for clinical dressing markets under outsourced freeze-drying scenarios.

Benefits to Industry

The project demonstrates that animal by-products can be upcycled into high-value wound care materials with enhanced healing properties, supporting industry goals in sustainability, waste minimisation, and diversification into biomedical markets. The technology provides a scientifically validated basis for future product development within the red meat and bio-based materials sectors.

3.0 Introduction

Wound healing is a complex, multistage biological process requiring the coordinated interaction of cells, growth factors, and extracellular matrix (ECM) components (Gurtner et al., 2008). In cases of extensive trauma, chronic wounds, or impaired healing (e.g., in diabetic ulcers), natural repair processes are insufficient, creating demand for advanced wound care materials. Collagen-based wound dressings are widely used in clinical practice, as they provide a protective barrier, maintain a moist environment, and act as a provisional ECM to promote tissue regeneration (Chattopadhyay & Raines, 2014). However, current dressings are not fully optimised to accelerate tissue regeneration or effectively modulate inflammation, resulting in suboptimal healing outcomes. Consequently, there is an unmet need for advanced collagen-based biomaterials that combine enhanced functionality with cost-effectiveness, sustainability and waste minimisation, while also delivering endogenous bioactives naturally present in animal-derived collagen, which are often absent in GMO-derived alternatives.

One of the critical limitations of existing collagen wound dressings is their inadequate customisation for specific healing phases. Commercial products often rely on Type I collagen alone, which provides structural stability but does not fully replicate the regenerative functions of Type III collagen (Wang et al., 2017). Type III collagen is abundant in early wound healing and is essential for tissue granulation, angiogenesis, cell migration, and wound contraction (Volk et al., 2011). It also contributes to immune modulation by regulating pro-inflammatory cytokines, thereby reducing scarring and improving overall tissue quality. Synthetic collagen analogues and engineered substitutes have been developed to reduce pathogen transmission risk, yet these often fail to mimic the mechanical, biochemical, and degradation properties of natural collagen, slowing integration and tissue regeneration (Lee et al., 2001; Chattopadhyay & Raines, 2014).

The main research question of this project is: can collagen wound dressing healing outcomes be enhanced by incorporating enzymatically derived Type III collagen peptides into collagen-based wound dressings, thereby improving tissue regeneration and cost-effectiveness through more efficient utilisation of the animal carcass? The basis of this work lies in the biological importance of Type III collagen in early wound repair and the potential to valorise underutilised by-products from the red meat industry into high-value medical applications. Our previous research on alkali-aided collagen extraction and encapsulation of bioactives into collagen matrices demonstrated promising results in simulated wound fluid models. However, encapsulation technologies are expensive, highlighting the need for a more cost-effective strategy, such as the direct incorporation of collagen peptides.

The primary target audience for this work could be the routine clinical wound care sector, where collagen-based dressings can be adopted with comparatively low regulatory and technical barriers. This segment provides the most practical and commercially accessible entry point, enabling early market adoption while generating information needed for subsequent expansion. Beyond this initial focus, the work also has strong relevance to clinicians treating chronic and trauma wounds, as well as to the biomaterials and biotechnology industries seeking sustainable, high-value solutions for advanced wound care. Chronic wounds alone affect approximately 420,000 Australians each year (Graves & Zheng, 2014), representing a substantial burden on healthcare systems, while trauma and surgical wounds remain a high-value but technically challenging market segment. For industry, the ability to transform low-value animal by-products into advanced wound care materials aligns with current priorities of sustainability, waste minimisation, and high-value product development in the red meat sector (Ramirez et al., 2021).

This project offers a combination of (i) enhanced wound healing applications, through the enrichment of Type III collagen peptides to better mimic native healing processes; (ii) sustainable processing, using environmentally responsible extraction methods with GRAS chemicals and valorisation of animal by-products; and (iii) a framework, where considerations of economic feasibility and scalability are integrated early alongside biological testing. The outcomes of this research are expected to provide insights into (i) the biological performance of novel collagen peptide-enriched dressings, (ii) preliminary production and cost estimates to guide considerations for scalability, and (iii) indicative pathways for market entry.

4.0 Project objectives

The following are the project objectives as stated in the contract:

1. Produce functional collagen peptides using optimized methods and the development of enhanced collagen-based wound dressings containing collagen peptides.
2. Evaluate performance and safety of collagen dressings.
3. Assess the financial feasibility of the wound dressing produced.

This final milestone report integrates the outcomes of all previous stages, encompassing the production and characterisation of functional collagen peptides, the development and optimisation of collagen-based wound dressing formats, the evaluation of their performance in 3D skin models for burn wound healing, and an economic feasibility analysis addressing scalability, production costs, and market potential.

5.0 Methodology

Milestone 1: Collagen Extraction and Characterisation

Collagen Extraction from Lamb Pelts and Lungs: Fresh lamb pelts and lungs were obtained from ANZCO Foods (Ashburton, New Zealand) and stored at $-20\text{ }^{\circ}\text{C}$ until processing. Collagen was extracted using a modified alkali extraction method. The extracted collagen from skin was freeze-dried to obtain a lightweight, fibrous mat that could be cut or torn without crumbling. Both skin- and lung-derived collagens were successfully extracted and freeze-dried. The collagen yield from lung tissue was higher than that from skin, likely due to differences in initial tissue composition and pre-processing.

Protein Characterisation by SDS–PAGE: Collagen extracts were analysed using SDS–PAGE to compare molecular composition with a commercial collagen standard (Sigma).

Densitometric Analysis: High-resolution gel images (400 dpi, 24-bit colour) were acquired using an Epson 3200 scanner (Japan) under transmission mode. Band quantification was performed using ImageQuant TL 1D software (GE Healthcare Life Sciences).

Milestone 2: Collagen Peptide Generation and Material Development

Peptide Generation from Lung Extract: Freeze-dried lung collagen was enzymatically hydrolysed. The enzyme was deactivated by heating at $95\text{ }^{\circ}\text{C}$ for 20 min.

Peptide Identification and LC–TIMS–MS/MS Analysis: Peptides and proteins were identified using liquid chromatography–trapped ion mobility spectrometry–tandem mass spectrometry (LC–TIMS–MS/MS). Data were searched against an in-house *Ovis aries* (sheep) protein database (42,954 sequences) with no enzyme specificity. Variable modifications included oxidation/hydroxylation (P), oxidation (M), pyro-glutamylation (Q), and deamidation (NQ). Identification thresholds were set at 1% false discovery rate (FDR) at the peptide level, $-10\text{LgP} > 20$ at the protein level, and ≥ 1 unique peptide per protein. Post-processing was conducted using PEAKS Online, with further analyses in R and Microsoft Excel 365.

Collagen Mat Fabrication and Crosslinking: Freeze-dried skin collagen (from Milestone 1) was rehydrated in deionised water (1.0% w/w) and homogenised (Ninja® Nutri-Blender Pro, 3 min). Crosslinking was achieved by reacting with genipin followed by incubation overnight at $4\text{ }^{\circ}\text{C}$. Residual genipin was quenched with lysine and re-incubated overnight at $4\text{ }^{\circ}\text{C}$. The resulting materials were frozen ($-80\text{ }^{\circ}\text{C}$, 5 h) and freeze-dried (3 days) to obtain collagen mats.

Mechanical Testing: Subsamples (8.0 mm diameter, ~ 3 mm thick) were punched from the mats and tested using a dynamic mechanical thermal analyser (DMTA, DMA 242 E Artemis, NETZSCH) in compression strain amplitude-sweep mode at $22\text{ }^{\circ}\text{C}$ and 1.00 Hz frequency. Strain amplitude ranged from 0.025% to 6.000%. Measurements were used to determine elastic modulus, mechanical stability, and the effects of potential genipin crosslinking.

Biodegradability Testing: Mats were incubated in simulated wound fluid (SWF) (Svensby et al., 2024) under controlled conditions ($37\text{ }^{\circ}\text{C}$, gentle agitation) for 5 days. Disc samples (3 mm \times 3 mm) were imaged daily using a Nikon D610 with a MicroNikkor 105 mm lens and SB-R200 flash system. Structural integrity and degradation patterns were visually and quantitatively assessed to evaluate material stability.

Microscopy Evaluation: Samples were sectioned under a stereomicroscope and mounted on SEM stubs using double-sided carbon tape. Surfaces and cross-sections were gold-coated (10 nm) using a DSR1 sputter coater (Nanostructured Coatings Ltd, Iran). Imaging was performed using a Hitachi 3030plus SEM (Tokyo, Japan) at 15 kV. Morphological features, fibre alignment, and porosity were analysed to assess structure–function relationships in untreated and genipin-crosslinked collagen mats.

Milestone 3: 3D skin model study

Skin Model: In this milestone, a full-thickness human skin model, EpiDermFT tissues (EFT-400-WHB; MatTek Corporation, Ashland, MA, USA) (Figure 1), was used. This model reproduces the primary layers of human skin, including the epidermis and dermis, but does not contain appendages such as hair follicles or glands. It is well-suited for evaluating local tissue compatibility, cytotoxicity, and molecular responses to various treatments.

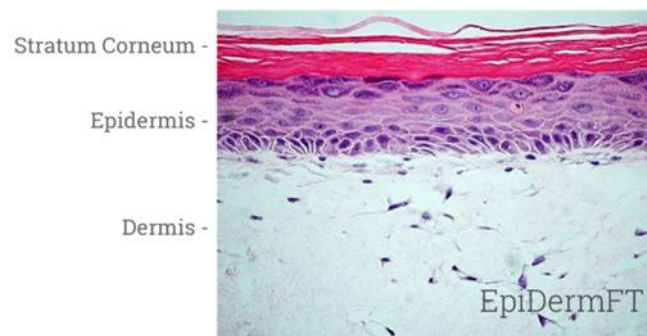


Figure 1 . Histology of EpiDermFT. The hematoxylin and eosin (H&E) stained paraffin section of EpiDermFT shows the epidermis containing basal, spinous, granular keratinocytes and stratum corneum. The dermis contains numerous viable fibroblasts. Source: MatTek Corporation.

To investigate the effects of collagen-based interventions, burned EpiDermFT tissues were utilised to assess the biological response. The burn model incorporates parallel epidermal burns, generated by the manufacturer using a cauteriser (Figure 2).



Figure 2. Image of burned 3D human skin tissues in a cell culture plate.

Four treatment groups were selected for detailed comparison

- No treatment (control)
- Collagen hydrolysate-infused mat
- Collagen hydrolysate solution
- Commercial collagen dressing

Collagen mats and hydrolysates were prepared according to Milestone 1 protocols.

Tissue Culture and Sampling: Upon receipt, tissues were transferred to 6-well plates containing 2.5 mL pre-warmed EFT-400-MM medium per well, equilibrated overnight at 37°C with 5% CO₂, and then allocated to treatments (Figure 3). Treatments were applied to apical surfaces, except human serum, which was delivered via culture medium. Media were refreshed daily, and conditioned media were stored at –80°C for cytokine analysis. Tissues were sampled daily for histology.



Figure 3. EpidermFT tissues being transferred from agarose gel (left hand plate) to culture medium (right hand plate) upon arrival from the manufacturer.

Histology: Tissues were fixed in 10% neutral-buffered formalin, sectioned to 6 μm , and stained with H&E and Masson's trichrome. Micrographs were obtained using a Leica D7 microscope. Trichrome staining enabled differentiation of epidermal and dermal compartments, with the epidermis staining red/purple and collagen-rich dermis blue (Figure 4).

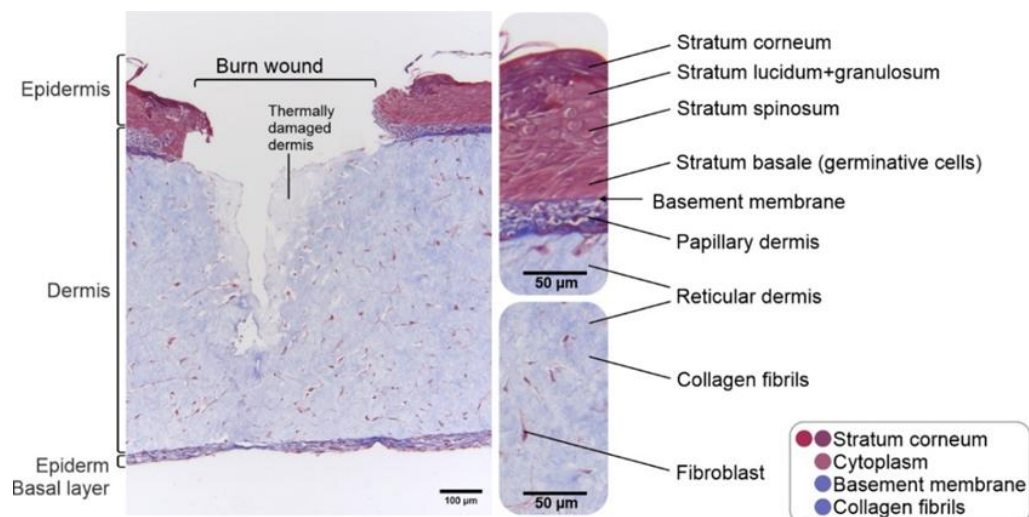


Figure 4. Burn wound tissue model general features with Masson's trichrome stain.

Cytokine Analysis: Cytokines were measured using the Milliplex Human High Sensitivity T Cell panel (HSTCMAG28SPMX13, Merck, Germany) based on Luminex xMAP technology, detecting GM-CSF, IFN- γ , IL-1 β , IL-2, IL-4, IL-5, IL-6, IL-7, IL-8, IL-10, IL-12(p70), IL-13, and TNF- α . Supervised multivariate analysis (OPLS-DA) was performed to assess treatment discrimination.

Scanning Electron Microscopy: Freeze-dried collagen mats and commercial dressings were sectioned, mounted on conductive stubs, coated with 10 nm gold, and imaged using a Hitachi 3030plus SEM at 15 kV. Surface and cross-sectional morphologies were assessed for porosity, fibril architecture, and hydrolysate incorporation.

Milestone 4: Economic Feasibility Assessment

A screening-level economic assessment of the collagen-based wound dressings was performed. While not a full techno-economic analysis (TEA), it integrated cost estimation, process flow, and scalability assessment using data generated in Milestones 1–2. The evaluation focused on production costs, scalability potential, and market positioning,

excluding detailed engineering design or clinical validation at this stage. The analysis assumed commercial viability based on expected superior wound-healing efficacy.

Cost and Process Modelling: Production cost estimates were derived from experimental yields of skin and lung collagen extractions. These data informed the development of a process flow diagram (PFD) and mass balance, outlining the key steps and material requirements. The study supported:

- Benchmarking against existing commercial collagen dressings.
- Estimated cost ranges and scalability potential

Investment-grade financial projections, validated engineering designs, or a defined commercialisation pathway were not attempted. Instead, an evaluation was carried out to determine whether the current research direction warrants continued development toward pilot-scale testing.

6.0 Results

In **Milestone 1**, the freeze-dried collagen obtained from sheep skin formed a lightweight, fibrous mat that could be torn or cut but remained cohesive under pressure (Figure 5). In contrast, the lung-derived collagen mat also formed a fibrous network but was more brittle, tending to crumble under applied pressure (Figure 6). This indicates differences in structural composition between skin- and lung-derived collagens.



Figure 5. Freeze-dried skin collagen mat.



Figure 6. Freeze-dried lung collagen mat.

The moisture content was low for both sources, with the skin collagen extract containing 1.1% and the lung extract 0.9% moisture, indicating effective dehydration post freeze-drying. Ash content differed substantially between the two

samples, with the lung extract containing 7.3% ash compared to 1.9% in the skin extract. This suggests a higher residual inorganic or mineral component in the lung-derived collagen, potentially reflecting inherent tissue composition.

Collagen was successfully extracted from both tissues. The yield from lung tissue (5.2%) was slightly higher than from pelt (4.3%), due to differences in the nature of the starting material. When adjusted for sample preparation (wool-on pelt vs trimmed lung), lung tissue demonstrated greater extraction efficiency under identical conditions.

Electrophoretic analysis confirmed the presence of major collagen Type I $\alpha 1$ and $\alpha 2$ chains in both extracts. In the lung extract, α -chain migration was slightly reduced, suggesting a marginally higher apparent molecular weight, potentially indicating post-translational modifications or differences in crosslinking.

In **Milestone 2**, collagen hydrolysate characterisation was reported. Gel permeation profiling of sheep lung hydrolysates showed a broad distribution of peptide sizes ranging from <100 Da to >10,000 Da (Figure 7). The majority of peptides were in higher molecular weight ranges: 36.1% between 1,000–10,000 Da and 33.4% above 10,000 Da. Low molecular weight peptides (<1,000 Da) accounted for 27.8% collectively. These results suggest that the enzymatic hydrolysis preferentially generated larger peptides.

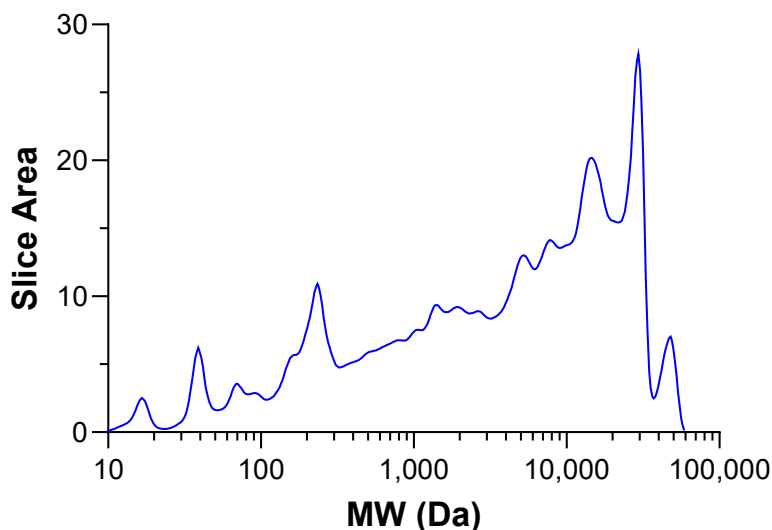


Figure 7. Molecular weight distribution of the sheep lung hydrolysate

Mass spectrometry identified 91 proteins and 5,783 unique peptides within the lung hydrolysate. The most abundant proteins, based on spectral counts, were elastin (17,059 spectra), collagen $\alpha 1(I)$, $\alpha 2(I)$, haemoglobin α -subunit, and collagen $\alpha 1(III)$. The high representation of collagen α -chains confirms the extract's origin, while the presence of elastin reflects the structural nature of lung extracellular matrix. The co-detection of Type I and III collagens indicate compositional complexity that could influence functionality in derived bio-based materials.

Dynamic mechanical thermal analysis (DMTA) showed that both untreated and genipin-treated collagen mats exhibited very low stiffness and strength, with modulus and force values near the instrument's detection limit (<1 mN). Although individual specimens displayed variability, no consistent differences in viscoelastic response were observed between treated and untreated samples. This indicates that genipin crosslinking did not substantially alter the bulk mechanical properties under the tested conditions (Figure 8).

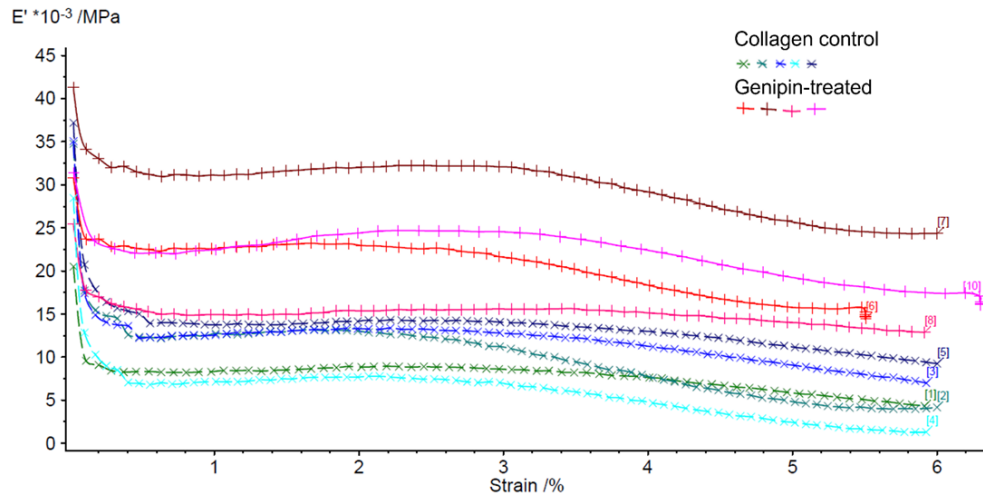


Figure 8: Storage moduli (E') as a function of strain amplitude (%) for 5 specimens each (see legend) of untreated collagen mat (*) and a genipin-treated collagen mat (+)

An in-house biodegradability test in simulated wound fluid, over a 5-day incubation at 37 °C, indicated that both untreated and genipin-treated mats maintained morphological integrity with minimal degradation. Untreated mats showed slight surface smoothing after 24 h, consistent with partial hydration or gelation, but no significant structural loss thereafter. Genipin-treated mats retained their compact morphology and exhibited a progressive colour shift (blue to violet), indicative of genipin-amino crosslink formation and subsequent oxidation (Hwang et al., 2011) (Figure 9), although the specific role of oxygen was not experimentally confirmed.

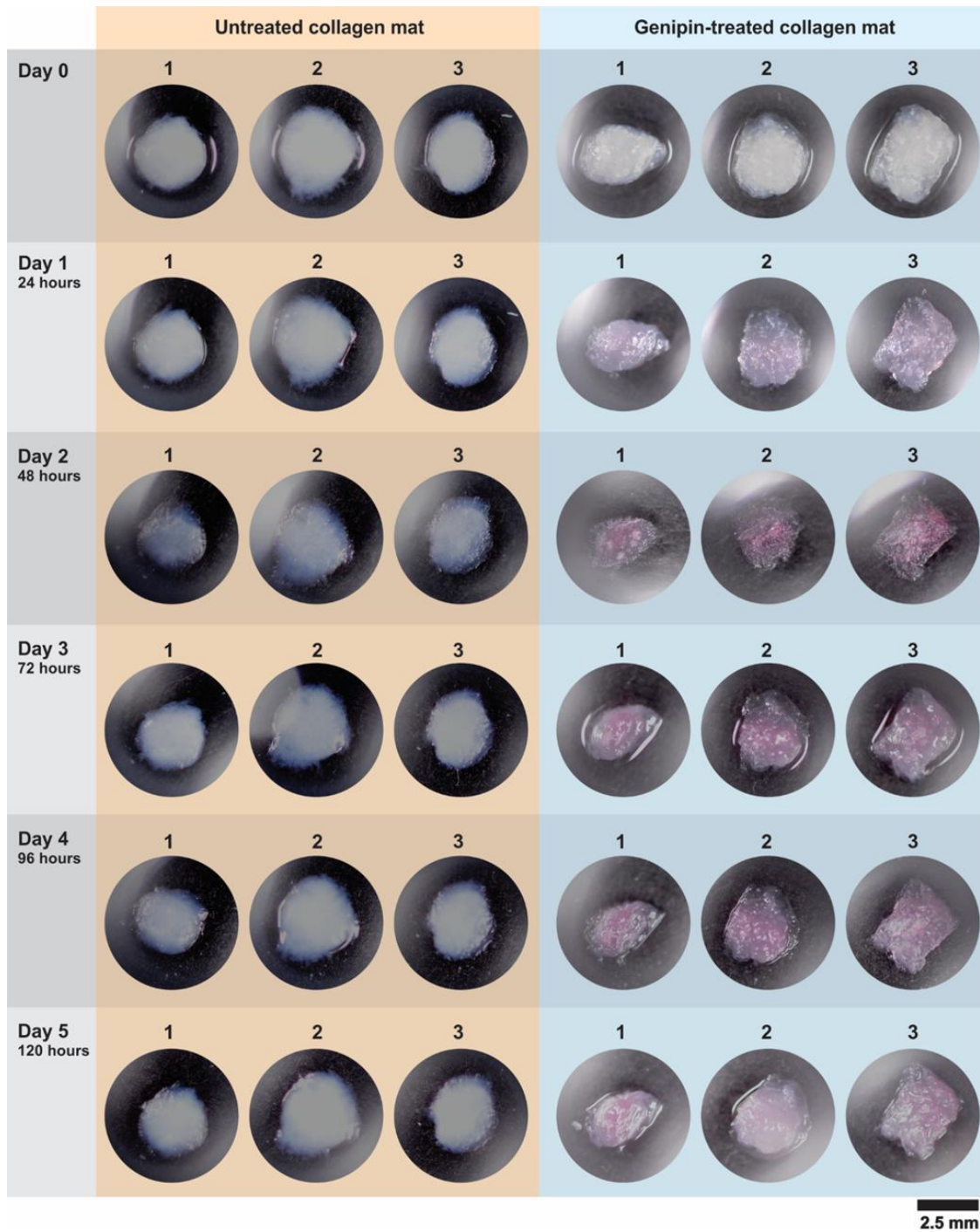


Figure 9. Untreated collagen mat and genipin-treated collagen mat incubated in simulated wound fluid at 37 °C. Incubation time ranging from 0-120 h.

Microscopy confirmed that untreated mats possessed an open, porous microstructure with fine, interconnected pores, while genipin-treated samples displayed smoother surfaces and larger, less densely packed pores (Figure 10).

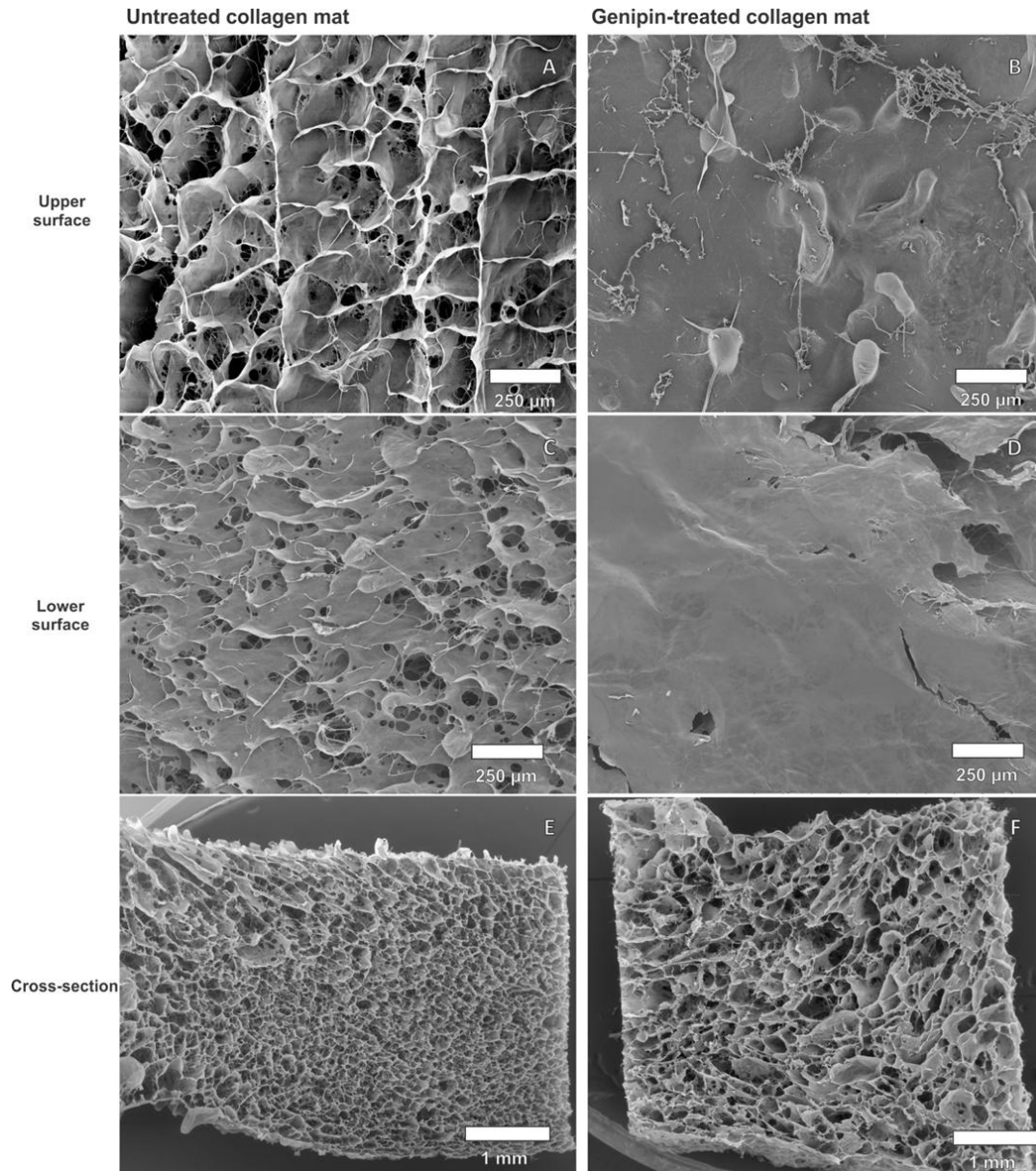


Figure 10. SEM images of the untreated collagen mat (A, C and E) and genipin-treated collagen mat (B, D and F). Mats were freeze-dried in a square petri dish and the upper surface (A and B), lower surface (i.e., the surface in contact with plastic during the freeze-drying step) (C and D) and cross-sections (E and F) were imaged.

In **Milestone 3**, we evaluated wound healing using 3D skin models. Histological evaluation and cytokine analysis of the skin models were performed to understand the healing process.

The EpiDermFT model exhibited progressive healing over six days. On receipt the burn models showed that the epidermis was completely ablated at baseline, and dermal damage appeared as cracks or holes surrounded by lighter staining due to thermal protein denaturation. In the no-treatment controls, the epidermal basal layer (Ep) and papillary dermis (PD) migrated into wounds from Day 1, forming a complete bridge by Day 3. Basement membrane (Bm) regeneration varied between samples, with complete layers observed by Day 6 in some tissues. Collagen fibrils were evident near PD margins. The collagen hydrolysate-infused mat exhibited healing responses that were comparable to or slightly better than the commercial mat. Re-epithelialisation and PD migration were consistent from Day 1, with variability in later-stage healing due to mat contact differences. Treatment with the commercial collagen mat displayed variable early responses; some samples showing delayed wound coverage. The peptide-only treatment produced a multicellular bridge and partial basement membrane by Day 1. Epidermis extended into dermis, and stratum corneum formation was observed by Days 4–5. Some early collagen deposition was noted (Figure 11). No treatments induced tissue toxicity.

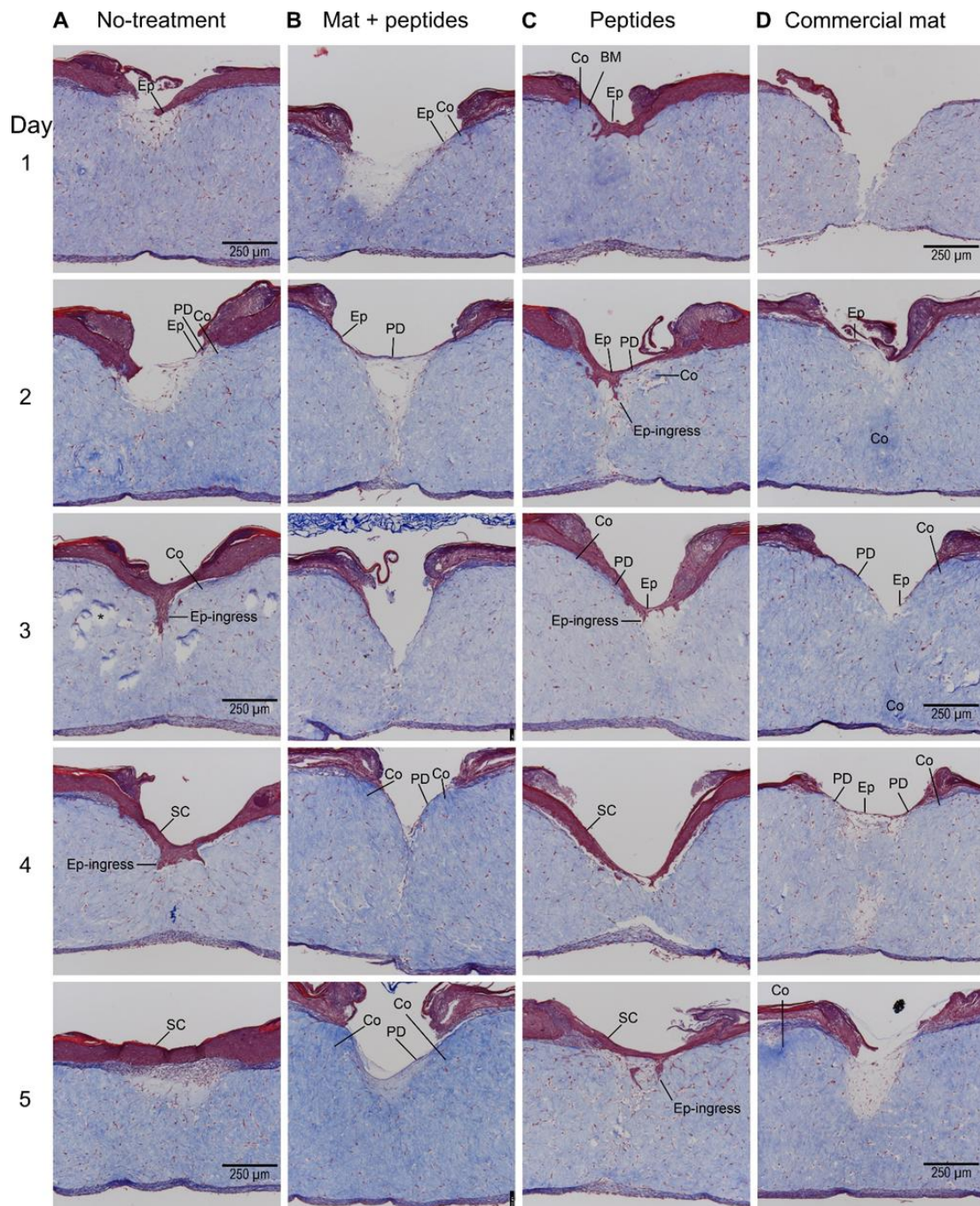


Figure 11. Histology matrix of treatment and days 1 to 5. Lines point to location of margins of cell layer migration into wound area (except where wound is fully bridged by a layer). Key: Co, collagen; Ep, epidermal cells; PD, papillary dermis; SC, stratum corneum. Scale bar is the same for all micrographs.

Cytokine profiling revealed the temporal dynamics of immune activation and tissue repair during wound healing, allowing assessment of biomaterial biocompatibility and comparative treatment efficacy (Figure 12). Rapid early spike in granulocyte-macrophage colony-stimulating factor (GM-CSF) was observed for collagen hydrolysate mat and solution, consistent with normal healing. The no-treatment control showed delayed elevation; commercial mat responses were mixed. Interferon γ showed an early rise post-burn in active treatments; muted in controls. Interleukin IL-1 β showed a modest increase in all groups, peaking Days 4–5; one no-treatment replicate showed an early burst. IL-10 peaked early in collagen hydrolysate treatments; muted response in commercial mat; delayed in controls. IL-10/IL-1 β ratio, indicated favourable anti-/pro-inflammatory balance for collagen hydrolysate treatments. Seven

cytokines (IL-2, IL-4, IL-5, IL-7, IL-12(p70), IL-13, TNF- α) showed no significant temporal or treatment-dependent variation.

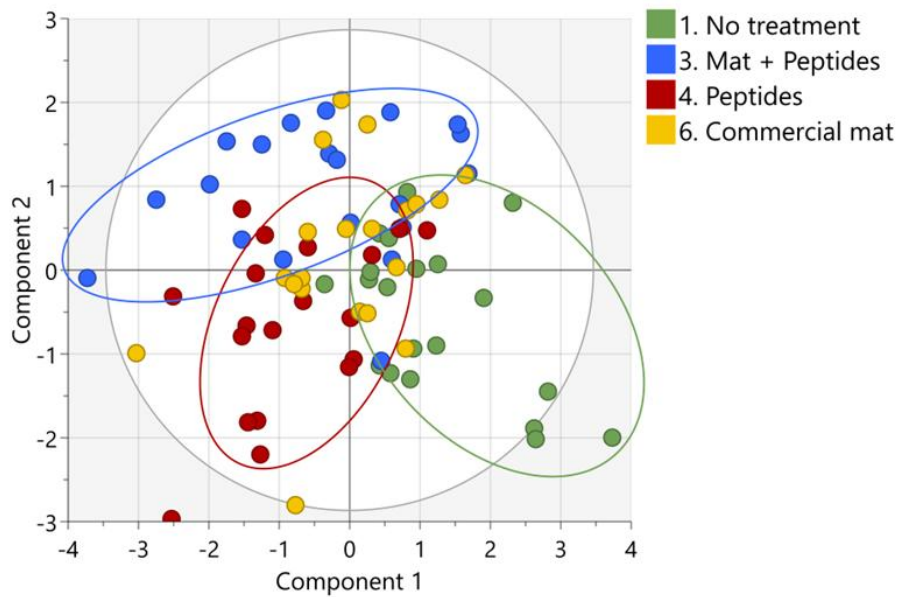


Figure 12. Score plot of OPLS-DA multivariate analysis of cytokine data. Ellipses enclosing most of the 'No treatment' (green), 'Mat + Peptides' (blue), and 'Peptides' (brick red) samples are overlaid to show the slight clustering of those treatments.

Scanning Electron Microscopy revealed an open, porous architecture with interconnected networks in the experimental collagen mats. Hydrolysate-infused mat exhibited additional surface deposits indicating peptide incorporation (Figure 13). The commercial mat had a distinct fibrillar structure (~30 μm fibrils with ~3 μm sub-fibrils), was less porous, and was markedly different from experimental mats (Figure 14).

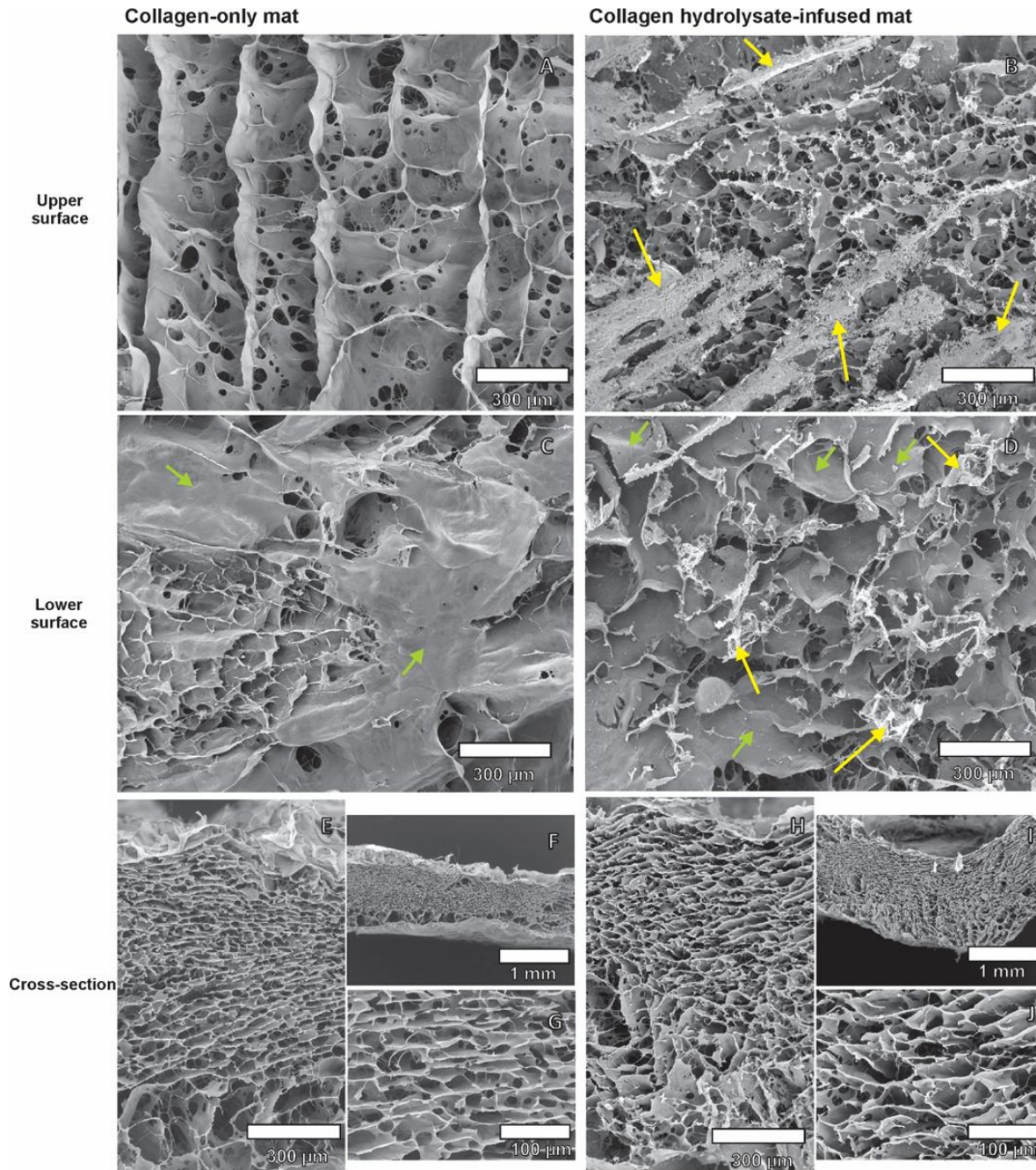


Figure 13. SEM images of the collagen-only mat (A, C and E-G) and collagen hydrolysate-infused mat (B, C and H-J). Mats were freeze-dried in a square petri dish and the upper surface (A and B), lower surface (i.e., the surface in contact with plastic during the freeze-drying step) (C and D) and cross-sections (E-J) were imaged. Green arrows indicate a smooth region on the lower surface (C and D) and yellow arrows indicate a material deposited on both the upper and lower surfaces on the collagen hydrolysate-infused mat (B and D).

Comfy Recombinant Collagen Dressing (a commercial collagen-based product)

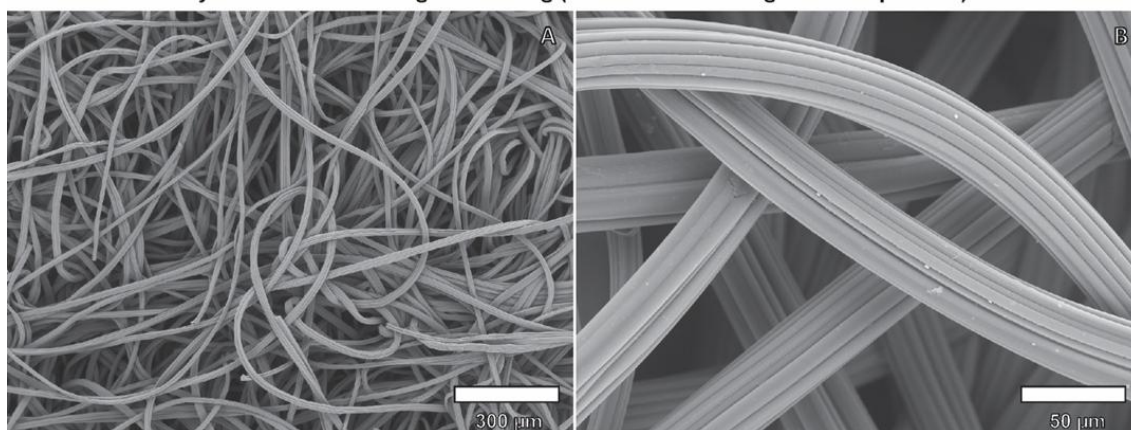


Figure 14. SEM images of the commercial collagen-based product (Comfy Recombinant Collagen Dressing).

The production feasibility and economic assessment were reported in **Milestone 4**. A process model integrating skin collagen and lung peptide extraction streams was developed. Production at pilot scale was constrained by freeze-dryer capacity (Cuddon FD600, 56 m² shelf area), allowing 54 m² of collagen mat per batch and an annual output of 4,860 m². Two production scenarios were assessed. In-house freeze-drying: production cost = AUD \$280/m²; annual production cost = \$1.37 M; capital investment = \$2.29 M. Outsourced freeze-drying: production cost = AUD \$200/m²; annual production cost = \$0.97 M; capital investment = \$0.59 M. Raw materials were dominated by potassium chloride (84% of cost) and sodium hydroxide (14%), suggesting opportunities for process optimisation or solution reuse to reduce input costs. Profitability analysis based on three proposed product concepts showed strong margins for medical applications.

- High-Needs Trauma Care: 99.8% gross margin; breakeven at 6 m² (12% of TAM).
- Routine Clinical Dressing: 80% gross margin; breakeven at 653 m² (6% of TAM).
- OTC Consumer Plasters: 20% gross margin; breakeven at 3,452 m² (12% of TAM).

The outsourced freeze-drying scenario demonstrated strong ROI for medical-grade applications (670–754%), allowing flexibility for further R&D spending while maintaining commercial viability.

The largest single cost component was the freeze-dryer, accounting for 87% of the total installed capital in the in-house scenario. Excluding this, the remaining process equipment cost was relatively modest (AUD \$98,000). Installation of a 100 m² cleanroom was estimated at \$325,000.

7.0 Discussion

A comprehensive interpretation of the results obtained across the project milestones, discussing their technical and practical significance for the development, application, and commercialisation of collagen-based wound dressings, is provided below:

In the first milestone, collagen was successfully extracted from both sheep skin and lung tissue using a modified alkali-based protocol. The comparable extraction efficiency between the two sources confirms the robustness and scalability of the developed process. The higher yield from lung tissue (5.2%) relative to pelt (4.3%) indicates that sheep lung may serve as a more efficient collagen source, particularly when considering its underutilisation within the red meat industry. The extraction workflow shows potential for further optimisation, which could increase yields even more across both tissue types. The observed textural differences in the freeze-dried materials, with lung collagen being more brittle and crumbly, likely reflect structural differences in fibrillar arrangement and crosslink density between dermal and pulmonary collagen.

The higher ash content in lung-derived collagen (7.3%) compared to skin (1.9%) suggests incomplete removal of non-collagenous components such as minerals, which may affect the purity of the final material. Further

optimisation of washing and neutralisation steps could improve chemical purity and standardise product quality, an important consideration for regulatory compliance and consistency in biomedical manufacturing.

Electrophoretic analysis demonstrated the presence of intact $\alpha 1$ and $\alpha 2$ chains with minimal degradation, confirming that the extraction process preserved the structural integrity of the collagen. The slower migration rate of α -chains in lung-derived collagen suggests a higher apparent molecular weight and supports the hypothesis of a greater Type III collagen content, consistent with the known composition of mammalian lung tissue.

This finding is significant because Type III collagen plays a critical role in early wound healing, supporting cell migration and granulation tissue formation. Therefore, lung-derived collagen may offer added biological performance compared to skin-derived collagen in regenerative applications. The near-equal intensity of $\alpha 1$ and $\alpha 2$ chains in the lung extract supports the presence of a mixed Type I/III collagen profile, aligning with the literature that places Type III at 20–30% of total lung collagen.

The demonstrated feasibility of collagen recovery from both sheep skin and lung validates the potential for valorising red meat by-products into high-value biomedical materials and supports waste minimisation goals within the meat processing sector.

In milestone 2, collagen peptide generation and mat development were reported. Enzymatic hydrolysis of lung collagen using Protease A generated predominantly medium- to high-molecular-weight peptides (1,000–10,000 Da), with limited quantities of smaller peptides. Although low-molecular-weight peptides are often more bioactive, this size distribution may still be advantageous for sustained release of bioactive fragments in a wound environment. In situ enzymatic activity (e.g., matrix metalloproteinases) in wound sites can further degrade these peptides, releasing smaller bioactive fragments that stimulate cell proliferation, angiogenesis, and collagen deposition. Thus, the current hydrolysate profile is well-suited for therapeutic application in collagen-based wound dressings. Mass spectrometry results indicated the presence of Type III collagen-derived peptides. Type III collagen is known to enhance early wound healing through fibroblast activation and extracellular matrix modulation (Stewart et al., 2025). The coexistence of Type I and Type III collagen peptides is expected to produce a potential additive effect, promoting both structural integrity and tissue regeneration. These findings justify advancing the hydrolysate into biological efficacy testing.

Microscopic evaluation revealed an open, interconnected pore structure in untreated collagen mats, which is ideal for tissue regeneration. Such morphology facilitates fluid absorption, oxygen diffusion, and cell infiltration which are key parameters for wound dressings (Gasper et al., 2011). Genipin-treated mats exhibited smoother, denser structures, potentially restricting these beneficial interactions. This structural difference explains why untreated mats were chosen for continued testing, as they balance mechanical stability with biological functionality.

Mechanical analysis confirmed that untreated mats possessed adequate elasticity and compressive strength for handling and application.

In biodegradation studies, both untreated and genipin-treated mats remained structurally intact after five days in simulated wound fluid (SWF). This stability is advantageous for short-term wound dressings, ensuring durability during the initial healing stages. The gradual hydration and partial gelation, expected in untreated mats may also support controlled peptide release, further enhancing their therapeutic potential.

The results from Milestone 2 demonstrate that a non-crosslinked collagen mat derived from sheep skin or lung is a technically viable wound dressing material. The material exhibits appropriate structural integrity and biodegradation rate for short-term wound care; has a morphology conducive to cell infiltration and fluid management; can be fabricated without chemical crosslinkers, simplifying manufacturing and regulatory compliance.

These characteristics make the technology particularly appealing for routine clinical dressing applications, where cost, ease of sterilisation, and biological compatibility are critical.

In milestone 3, the integrated histological and cytokine analysis was reported to provide a comprehensive view of wound repair dynamics in the EpiDermFT full-thickness skin model, highlighting differential effects among the treatments. The peptide-only treatment elicited a rapid early-stage healing response, evidenced by accelerated epidermal migration, basement membrane formation, and reorganisation of dermal collagen. The collagen

hydrolysate-infused mat and peptide solution treatments promoted timely, coordinated cytokine responses, including GM-CSF, IFN- γ , IL-1 β , and IL-10, reflecting activation of effective inflammatory and repair pathways. Together, these observations indicate that the experimental collagen mat supports wound healing dynamics comparable to, or in some aspects, more beneficial than, the commercial collagen dressing.

In contrast, the commercial collagen dressing induced weaker and more variable cytokine responses, potentially due to its fibrillar morphology and unavailability of soluble bioactive peptides. These findings suggest that the microscopic interface between the mat and the tissue, as well as the internal architecture of the scaffold, may influence functional performance. The open, porous structure and hydrolysate enrichment of the experimental mat likely enhanced cellular interaction, contributing to a more reliable repair response, although this conclusion is based on a limited number of replicates.

No-treatment controls provided a baseline, demonstrating the model's capacity for re-epithelialisation and dermal remodelling. While visually robust epidermal healing was observed, cytokine profiles indicated delayed and inconsistent activation of key inflammatory and repair mediators relative to the collagen treatments. Collagen mat formats can also provide mechanistic advantages by offering a structural scaffold and sustained delivery of bioactive peptides, supporting cellular migration, proliferation, and extracellular matrix deposition.

Overall, the milestone study demonstrated that controlled incorporation of collagen hydrolysates or peptides enhances wound healing at both structural and molecular levels. These data support the potential of peptide-enriched collagen biomaterials as next-generation scaffolds or topical therapeutics, enabling accelerated epidermal regeneration while maintaining a balanced inflammatory response.

In milestone 4, an economic feasibility analysis was performed. The economic evaluation revealed distinct opportunities and challenges across the proposed product concepts:

- High-Needs Trauma Care, although showing strong potential return on investment (ROI), entry barriers are significant due to regulatory and clinical validation requirements. This segment would necessitate strategic partnerships with medical device manufacturers and hospital networks.
- Routine Clinical Dressing, represents the most pragmatic and economically viable entry point. Regulatory pathways are clearer, development costs are moderate, and clinical familiarity with collagen dressings is already established. With demonstrated performance improvements, this category offers the most favourable ROI and earliest market access.
- OTC/Consumer Products, characterised by low margins and high-volume requirements, this segment may only become feasible once production is fully scaled and unit costs are minimised. Simplified formulations that avoid freeze-drying could be developed for this market tier in future.

Cost modelling identified freeze-drying as a major operational expense and capacity-limiting step. Comparative analysis of in-house vs. outsourced freeze-drying suggested that while outsourcing may reduce short-term costs, it introduces potential risks related to compliance, quality control, and supply chain security. For medical-grade applications, maintaining in-house processing is likely necessary to ensure consistent quality and regulatory assurance. The production rate model, based on a Cuddon FD600 freeze-dryer operating 90 batches per year, yielded an estimated annual capacity of 4,860 m² of collagen mat, sufficient for commercial pilot operations. Future optimisation of the drying process or adoption of alternative dehydration methods (e.g., air or vacuum drying) could substantially reduce costs and expand market accessibility.

The economic assessment indicates that the routine clinical dressing market offers the strongest balance between feasibility, profitability, and impact. A phased approach is recommended:

- Short-term: Focus on routine clinical dressings and low-cost OTC plasters. These segments have lower regulatory and development barriers, allowing pilot-scale production and clinical validation to be achieved efficiently. Early adoption in these markets provides a foundation for clinical credibility and market presence.
- Medium- and Long-term: Expand into trauma-grade products, which present higher technical and regulatory challenges. Entry into this segment will benefit from established partnerships with healthcare manufacturers, comprehensive clinical evidence, and scaled production capabilities. While the ROI is potentially high, development costs and market entry barriers are significantly greater than for routine or OTC dressings.

8.0 Conclusions

This project successfully demonstrated the feasibility of extracting and developing functional collagen-based biomaterials from underutilised red meat by-products, specifically sheep skin and lung tissue. The outcomes across all milestones establish a strong foundation for the applied development of collagen-derived wound care materials.

From Milestone 1, the modified alkali-based extraction method effectively yielded high-quality collagen from both sheep skin and lung tissue. While both extracts formed lightweight fibrous mats, the lung-derived collagen exhibited a more brittle texture and higher ash content, indicating intrinsic compositional differences compared with skin-derived collagen. SDS-PAGE analysis confirmed the presence of both type I and type III collagen, with lung tissue particularly enriched in type III, a collagen type strongly associated with early-stage tissue regeneration and wound healing. These findings support the use of lung tissue as a viable collagen source for biomedical applications with its higher proportion of type III collagen complementing the properties of type I collagen typically derived from skin.

Milestone 2 advanced this work by generating collagen peptides and developing collagen-based mat formats suitable for wound healing. The peptide analysis confirmed that the lung extract is rich in type III collagen peptides, suggesting intrinsic bioactivity relevant to tissue repair. Mechanical and biodegradability testing demonstrated that untreated collagen mats possessed adequate elasticity, compressive strength, and morphological stability under simulated wound conditions. Importantly, treatment with genipin did not significantly enhance performance, indicating that simpler, non-crosslinked mats are sufficient for practical handling and functional use. The open, porous structure of these untreated mats supports cell infiltration, fluid absorption, and gradual peptide release, key properties for promoting healing in dynamic wound environments. These findings identify non-crosslinked, peptide-enriched collagen mats as strong candidates for the next phase of biological validation using 3D skin models.

In Milestone 3 the reconstructed full-thickness skin model effectively captured key structural and functional aspects of human skin, allowing detailed evaluation of epidermal and dermal responses to different treatments. Across all analyses, the collagen mat incorporating bioactive peptides was shown to safely support wound healing without causing additional tissue damage or inhibiting repair processes. Histological assessment revealed that this treatment promoted consistent migration of the epidermal and papillary dermal layers into the wound region, while cytokine profiling demonstrated timely activation of critical inflammatory and repair mediators, including GM-CSF, IFN- γ , IL-1 β , and IL-10. These reflect a coordinated inflammatory response and effective tissue regeneration comparable to, and in some respects more reliable than, the commercial collagen mat. The peptide solution treatment further confirmed that soluble bioactive peptides can accelerate early-stage wound repair, with rapid formation of multicellular epidermal bridges and partial basement membrane reconstruction observed as early as day 1.

Microscopy evaluation of the collagen mats highlighted the functional relevance of scaffold architecture, with porous, open structures supporting tissue integration and hydrolysate-enriched surfaces likely enhancing bioactive interactions. In contrast, the commercial mat's fibrillar morphology and lower porosity may contribute to slower or less consistent early-stage responses. Collectively, these findings indicated that collagen-based biomaterials enriched with bioactive peptides offer both structural and molecular advantages, providing a scaffold for tissue regeneration and sustained peptide delivery. This dual functionality positions these materials as promising candidates for regenerative medicine and advanced wound care, with the potential to improve healing outcomes, particularly in chronic or complex wound scenarios.

In Milestone 4 an economic feasibility assessment was performed, identifying "Routine Clinical Dressing" as the most practical and strategically viable initial market entry point. This product category aligns well with existing regulatory frameworks and demonstrates a favourable return on investment (ROI) under realistic production scenarios. In contrast, "High-Needs Trauma Care" offers higher potential margins but faces considerable regulatory and clinical validation hurdles, while "OTC/Consumer Plasters" would require significant process optimisation to achieve cost competitiveness. Freeze-drying was identified as the primary cost driver; therefore, optimisation of drying methods, chemical use, and process efficiency will be critical for scalability and cost reduction.

From an industry and application standpoint, this project establishes a practical route for converting low-value by-products from the red meat sector into functional, high-value biomedical materials. The approach supports sector sustainability objectives by adding value to existing waste streams. The demonstration that non-crosslinked, type III-rich collagen mats are both structurally stable and amenable to fabrication provides a strong foundation for advancing toward prototype development and pilot-scale validation in partnership with industry stakeholders.

9.0 Project outputs

Collagen mat prototype display at the AMPC Innovation Showcase 2025, Brisbane.

10.0 Bibliography

Chattopadhyay, S. & Raines, R.T. (2014) 'Collagen-based biomaterials for wound healing', *Biopolymers*, 101(8), pp. 821–833. doi: 10.1002/bip.22486.

Gaspar, A., Moldovan, L., Constantin, D., Stanciuc, A.M., Sarbu Boeti, P.M. & Efrimescu, I.C. (2011) 'Collagen-based scaffolds for skin tissue engineering', *Journal of Medicine and Life*, 4(2), pp. 172–177.

Graves, N. & Zheng, H. (2014) 'Modelling the direct health care costs of chronic wounds in Australia', *Wound Practice and Research*, 22(1), pp. 20–33.

Gurtner, G.C., Werner, S., Barrandon, Y. & Longaker, M.T. (2008) 'Wound repair and regeneration', *Nature*, 453(7193), pp. 314–321. doi: 10.1038/nature07039.

Hattori, S., Adachi, E., Ebihara, T., Shirai, T., Someki, I. and Irie, S., 1999. Alkali-treated collagen retained the triple helical conformation and the ligand activity for the cell adhesion via $\alpha 2\beta 1$ integrin. *Journal of Biochemistry*, 125(4), pp.676–684.

Hwang, Y.J., Larsen, J., Krasieva, T.B. & Lyubovitsky, J.G. (2011) 'Effect of genipin crosslinking on the optical spectral properties and structures of collagen hydrogels', *ACS Applied Materials & Interfaces*, 3(7), pp. 2579–2584. doi: 10.1021/am200416h.

Lee, C.H., Singla, A. & Lee, Y. (2001) 'Biomedical applications of collagen', *International Journal of Pharmaceutics*, 221(1–2), pp. 1–22. doi: 10.1016/S0378-5173(01)00691-3.

Ramirez, J., McCabe, B., Jensen, P., Speight, R., Harrison, M., van den Berg, L. & O'Hara, I. (2021) 'Wastes to profit: a circular economy approach to value-addition in livestock industries', *Animal Production Science*, 61(6), pp. 541–550.

Stewart, D.C., Brisson, B.K., Yen, W.K., Liu, Y., Wang, C., Ruthel, G., Gullberg, D., Mauck, R.L., Maden, M., Han, L. & Volk, S.W. (2025) 'Type III collagen regulates matrix architecture and mechanosensing during wound healing', *Journal of Investigative Dermatology*, 145(4), pp. 919–938.e14. doi: 10.1016/j.jid.2024.08.013.

Svensby, A.U., Nygren, E., Gefen, A., Cullen, B., Ronkvist, Å.M., Gergely, A. & Craig, M.D. (2024) 'The importance of the simulated wound fluid composition and properties in the determination of the fluid handling performance of wound dressings', *International Wound Journal*, 21(5), e14861. doi: 10.1111/iwj.14861.

Volk, S.W., Wang, Y., Mauldin, E.A., Liechty, K.W. & Adams, S.L. (2011) 'Diminished type III collagen promotes myofibroblast differentiation and increases scar deposition in cutaneous wound healing', *Cells Tissues Organs*, 194(1), pp. 25–37. doi: 10.1159/000322399.

Wang, Y., Beekman, J., Hew, J., Jackson, S., Issler-Fisher, A.C., Parungao, R., Lajevardi, S.S., Li, Z. & Maitz, P.K. (2017) 'Burn injury: Challenges and advances in burn wound healing, infection, pain and scarring', *Advanced Drug Delivery Reviews*, 123, pp. 3–17. doi: 10.1016/j.addr.2017.09.018.